PUNE RESEARCH WORLD ISSN 2455-359X
AN INTERNATIONAL JOURNAL OF INTERDISCIPLINARY STUDIES VOL 2, ISSUE 2

EFFECT OF SUCTION ON THE FREE CONVECTIVE HEAT TRANSFER THROUGH A POROUS MEDIUM IN A CONCENTRIC ANNULUS

DR. K. GNANESWAR
Principal, S.K.P. Government Degree College,
Guntakal, Anantapuramu-Dist, **(TN) INDIA**

ABSTRACT

In this title we have presented the effect of radiation on mixed convective heat transfer flow of a viscous electrically conducting fluid through a porous medium confined in a porous cylindrical annulus under radial magnetic field. The equations governing the flow and heat transfer have been solved by using Gauss Seidel iteration method. The velocity and the temperature have been analyzed for different values of G, D-1, M, , and . Also stress and the rate of heat transfer on the inner and outer cylinders have been numerically evaluated.

Keywords: *Suction; Convective Heat transfer; Porous medium; Concentric annulus; Finite Element Method.*

1. INTRODUCTION

Many processes in engineering areas occur in high temperatures are consequently the radiation plays a significant role. Chandrasekhara and Nagaraju [5] examined the composite heat transfer in a variable porosity medium bounded by an infinite vertical flat plate in the presence of radiation. Yih [32] studied the radiation effects on natural convection over a cylinder embedded in porous media. Mohammadien and El-Amin [15] considered the thermal radiation effects on power law fluids over a horizontal plate embedded in a porous medium. Raptis [25] studied the steady flow heat transfer in a porous medium with high porosity in the presence of radiation.

It has been established from experiment and theoretical studies the laminarization of the boundary layer over a profile reduces the drag and hence the energy requirements by a very substantial amount, one of the ways in which a turbulent may be suppressed is, to remove mass from the boundary layer through pores or slits on the boundary. The development on this subject has been compiled by Lachaman [12].An important design consideration in such

a profile is the geometry and configuration of the outlets through which the suction is affected.

The study of flow and heat transfer in the annular region between the concentric cylinders has applications in nuclear waste disposal research. It is known that canisters filled with radio active rays be buried in the earth so as to isolate to determine the surface temperature of this canisters. This surface temperature strongly depends on the buoyancy driven flow sustained by the heated surface and the possible moment of ground water past it. This phenomenon make idealized to the study of convection flow in a porous medium contained in a cylindrical annulus and extensively has been made on these lines [20-22]. To obtain any desired reduction in the drag increasing suction alone is uneconomical as the energy consumption of the suction pump will be more. Therefore the methods of 'cooling of the Wall' in controlling the laminar flow together with the application of suction has become more useful.

Free convection in a vertical porous annulus has been extensively studied by Prasad [21], Prasad and Kulacki [22] and Prasad et al. [20] both theoretically and experimentally. Caltagirone [4] has published a detailed theoretical study of free convection in a horizontal porous annulus, including possible three dimensional and transient effects. Similar studies for fluid filled annuli are available in the literature [24]. Convection through annular regions under study conditions has been discussed with the two cylindrical surfaces left at different temperatures [12]. This work has been extended in temperature dependent convection flow [7,8,14] as well as convection flows through horizontal porous channel whose inner surface is maintained at constant temperature, while the other surface is maintained at circumferentially varying sinusoidal temperature [16,26,32]. Free convection flow and heat transfer in hydro magnetic case is important in nuclear and space technology [14, 18, 19, 29, 34, and 35]. In particular such convection flow in a vertical annulus region in the presence of radial magnetic field has been investigated by Sastry and Bhadram [28].Murthy [31] has analyzed the free convection flow of an incompressible, viscous, electrically conduction fluid through a porous medium in the annulus between the concentric cylinders under the influence of a radial magnetic field. Sivanjaneya Prasad [30] has investigated the free convection flow of an incompressible, viscous fluid through a porous medium in the annulus between the porous cylinders under the influence of a radial magnetic field. Antonio [2] has investigated the laminar flow heat transfer in a vertical circular duct by taking into account both viscous dissipation and the effect of buoyancy. The limiting case of fully developed natural convection in porous annuli is solved analytically for study and transient cases by El-Sharawi and Al- Nimir [6, 1]. Philip [18] has obtained analytical solution for the annular porous media valid for low modified Reynolds number.

Yih [32] has studied the effect of radiation on natural convection over a vertical cylinder using finite difference method. Hossain and Alim [9] have investigated the natural convection radiation interaction on the boundary layer flow along vertical cylinder by using

two different methods i.e., local non similarity method and implicit finite difference scheme with keller box elimination method. The porous medium embedded in vertical annular cylinder is an important area which finds engineering applications in heat exchangers, insulated pipe lines, gas cooled reactor vessels, bio-mass converters etc., Rajamani et al. [23] have studied the natural convective heat transfer in an annular cylinder .Irfan Anjum, Badruddin et al [10] have studied the effect of viscous dissipation and radiation on natural convection in a porous medium embedded within vertical annulus.

2. FORUMLATION OF THE PROBLEM

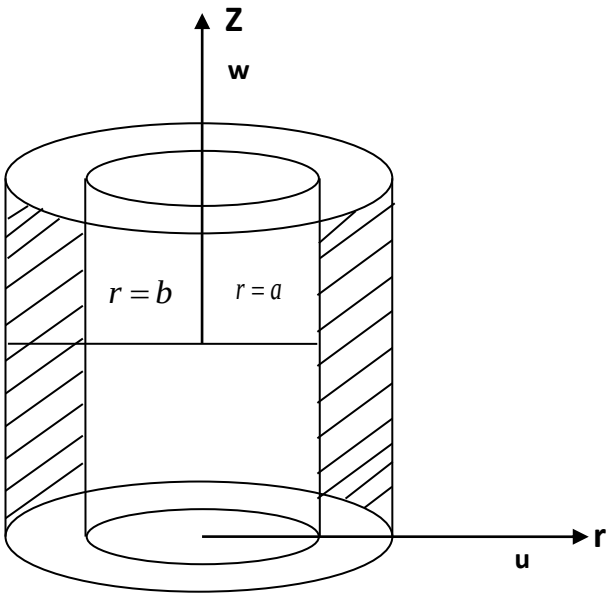

Fig.2 : Schematic diagram of the flow configuration

We consider the fully developed, steady laminar free convective flow of an incompressible, viscous, electrically conducting fluid through a porous medium in a annular region between two vertical co-axial porous circular pipes. We choose the cylindrical polar coordinates system O (r, θ , z) with the inner and outer cylinders at r = a and r = b respectively. The inner wall is maintained at constant temperature and the outer wall is maintained at constant heat flux. The fluid is subjected to the influence of a radial magnetic field (H_0 / r). Pipes being sufficiently long all the physical quantities are independent of the axial coordinate Z. The fluid is chosen to be of small conductivity so that the Magnetic Reynolds number is much smaller than unity and hence the induced magnetic field is negligible compared to the applied radial field. Also the motion being rotationally symmetric the azimuthal velocity V is zero. The equation of motion governing the MHD flow through the porous medium are

$$u_r + u / r = 0 \tag{3.1}$$

$$\rho_e u u_r = - p_r + \mu (u_{rr} + u_r / r - u / r^2) - (\mu / k) u \tag{3.2}$$

$$\rho_e u w_r = - p_z + \mu (w_{rr} + w_r / r) - (\mu / k) w - \rho g - (\sigma \mu_e^2 H_0^2 a^2 / r^2) w \tag{3.3}$$

$$\rho C_p (u T_r) = k_1 (T_{rr} + T_r / r) + \mu \left[2 (u_r^2 + u^2 / r^2) + w_r^2 \right] + (\mu / k + \sigma \mu_e^2 H_o^2)(u^2 + w^2) + Q - \frac{1}{r} \frac{\partial (r q_r)}{\partial r} \tag{3.4}$$

$$\rho - \rho_e = - \beta (T - T_0) \tag{3.5}$$

where (u ,w) are the velocity components along 0 (r ,z) directions respectively, ρ is the density of the fluid, p is the pressure, T is the temperature, μ is the

Coefficient of viscosity , C_p is the specific heat at constant pressure , k is the porous permeability, σ is the electrically conductivity, μ_e is the magnetic permeability and ρ_e, T_e are density, temperature in the equilibrium state. Where k_1 is the coefficient of thermal conductivity, Q is the strength of the heat source/sink (suffices r and z indicate differentiation w.r.t the variables).

The boundary conditions are

$$w(a) = w(b) = 0 \tag{3.6}$$

$$T(a) = T_i \text{ and } \frac{dT}{dr} = Q_1 \ at \quad r = b \tag{3.7}$$

The equation of continuity gives

$$r u = a u_a = b u_b$$

$$\Rightarrow \quad u_b = (a / b) u_a \tag{3.8}$$

In the hydrostatic state equation (3.3) gives

$$- \rho_e g - p_{e,z} = 0 \tag{3.9}$$

where ρ_e and p_e are the density and pressure in the static case and hence

$$- \rho g - p_z = - (\rho - \rho_e) g - p_{d,z} \tag{3.10}$$

where p_d is the dynamic pressure

Also substituting (3.10) in (3.2) we find

$$\frac{\partial p_d}{\partial r} = f(r) \qquad (3.11)$$

Using the relation (3.9) – (3.11) in (3.1) – (3.4) the equations governing free convective heat transfer flow under no pressure gradient are

$$w_{rr} + (1 - a u_a / \nu)\, w_r / r + ((\beta g / \nu)(T - T_e)$$
$$(\sigma \mu_e^2 H_0^2 a^2 / \nu)\ (w / r^2) - (\nu / k)\, w = 0 \qquad (3.12)$$

$$T_{rr} + (1 - a u_a / \nu) T_r / r + \mu(2(u^2 / r^2) + w_r^2) + (\mu / k + \sigma \mu_e^2 H_o^2)(u^2 + w^2) + Q = 0 \qquad (3.13)$$

Introducing the non-dimensional variables

$$(r', w', \theta') \text{ as } r' = r/a\ ,\ w' = w(a/\nu)\ ,\quad \theta = \frac{T - T_e}{T_i - T_e} \qquad (3.14)$$

the equations (3.12) and (3.13) reduce to

$$w_{rr} + (1 - \lambda)(1/r)\, w_r - (D_2^{-1} + (M^2 / r^2))\, w = -G\theta \qquad (3.15)$$

$$\theta_{rr} + (1 - \lambda)\theta_r / r = -PE_c(w_r^2 + \lambda^2 / r^4) + \alpha \qquad (3.16)$$

where $M = (\sigma \mu_e^2 H_0^2 a^2 / \rho \nu)^{1/2}$ (the Hartmann number)

$G = (\beta g a^3 (T_1 - T_e)^2 / \nu^2)$ (the Grashoff number)

$\lambda = a u_a / \nu$ (the Suction parameter)

$D_2^{-1} = (a^2 / k)$ (the Darcy parameter)

$P = (\mu C_p / k_1)$ (the Prandtl number)

$E_e = (\nu / k_1 a^2 (T_i - T_e))$ (the Eckert number)

$\alpha = \frac{QL^2}{k_1}$ (the Heat Source parameter)

The corresponding boundary conditions are

$w = 0\ ,\ \theta = 1\ ,$ on $r = 1$

$$w = 0\,, \quad \frac{d\theta}{dr} = Q_1 \quad \text{on} \quad r = s \tag{3.17}$$

where $m_1 = \dfrac{T_o - T_e}{T_i - T_e}$

Assuming Ec<<1, we take the solution as

$$w = w_0 + Ec\, w_1 + \ldots\ldots\ldots\ldots$$

$$\theta = \theta_0 + Ec\, \theta_1 + \ldots\ldots\ldots\ldots\ldots \tag{3.18}$$

Substituting (3.16) in equations (3.12) and (3.13) and separating the like powers of Ec

The equations to the zeroth order are

$$w_{o,rr} + (1-\lambda)(1/r)w_{0,r} - (D_2^{-1} + \frac{M^2}{r^2})w_0 = -G\theta_o \tag{3.19}$$

$$\theta_{0,rr} + (1-\lambda P_1)(1/r)\theta_{0,r} + \alpha_1 = 0 \tag{3.20}$$

and to the first order are

$$w_{1,rr} + (1-\lambda)(1/r)w_{1,r} - (D_2^{-1} + \frac{M^2}{r^2})w_1 = -G\theta_1 \tag{3.21}$$

$$\theta_{1,rr} + (1-\lambda P_1)(1/r)\theta_{1,r} = -P_1(w^2{}_{o,r} + \lambda^2/r^4) \tag{3.22}$$

The corresponding boundary conditions are

$$w_0(1) = 0\,,\ w_0(s) = 0, \tag{3.23}$$

$$\theta_0(1) = 0\,, \quad \frac{d\theta_0}{dr} = Q_1 \quad \text{on } r = s \tag{3.24}$$

and

$$w_1(1) = 0\,,\ w_1(s) = 0, \tag{3.25}$$

$$\theta_1(1) = 0\,, \quad \frac{d\theta_1}{dr} = 0 \quad \text{on } r = s \tag{3.26}$$

The differential equations (3.17)-(3.20) have been discussed numerically by reducing the differential equations into difference equations which are solved using Gauss-Seidel Iteration

method. The differential equations involving θ_0, θ_1, W_0 and W_1 are reduced to the following difference equations

$$\left(1-\frac{h(1-\lambda P_1)}{2r_i}\right)\theta_{0,i-1}-2\theta_{0,i}+\left(1+\frac{h(1-\lambda P)}{2r_i}\right)\theta_{0,i+1}=-\alpha_1 h^2 \tag{3.27}$$

$$\left(1-\frac{h(1-\lambda)}{2r_i}\right)w_{0,i-1}-\left(2+h^2\left[D_2^{-1}+(M^2/r^2)\right]\right)w_{0,i}+\left(1+\frac{h(1-\lambda)}{2r_i}\right)w_{0,i+1} = -Gh^2(\theta_{0,i}) \tag{3.28}$$

$$\left(1-\frac{h(1-\lambda P_1)}{2r_i}\right)\theta_{1,i-1}-2\theta_{1,i}+\left(1+\frac{h(1-\lambda P_1)}{2r_i}\right)\theta_{1,i+1} = P_1 h\left(\lambda^2/r^4+w^2{}_{0,r}\right). \tag{3.29}$$

$$\left(1-\frac{h(1-\lambda)}{2r_i}\right)w_{1,i-1}-\left(2+h^2\left[D_2^{-1}+(M^2/r^2)\right]\right)w_{1,i}+\left(1+\frac{h(1-\lambda)}{2r_i}\right)w_{1,i+1} = -Gh^2(\theta_{1,i})$$

$$(i=1, 2,\ldots\ldots\ldots\ldots\ldots\ldots\ldots..21) \tag{3.30}$$

where h is the step length taken to be 0.05 together with the following conditions

$$w_{0,0}=0, \quad w_{0,17}=0$$
$$w_{1,0}=0, \quad w_{1,17}=0$$

All the above difference equations are solved using Gauss-Seidel iterative method to the fourth decimal accuracy.

The shear stress on the pipe is given by

$$\tau' = \mu\left(\frac{\partial w}{\partial r}\right)_{r=a,b}$$

which in the non-dimensional reduces to

$$\tau = \tau'/(\mu^2/a^2) = (w_r)_{r=1,s} = (w_{0,r}+E_e w_{1,r})_{r=1,s}$$

The heat transfer through the pipe to the flow per unit area of the pipe surface is given by

$$q = k_1(\frac{\partial T}{\partial r})_{r=a,b}$$

which is in the non-dimensional form is $$Nu = \frac{qa}{k_1(T_1 - T_e)} = \left(\frac{\partial \theta}{\partial r}\right)_{r=1,s}$$

3. NUMERICAL RESULTS

In this analysis we investigate the Convective Heat transfer of viscous, electrically conducting fluid through a porous medium in the circular annulus between two porous cylinders at r = a and r = b. The outer cylinder is maintained at a constant heat flux and the inner wall is maintained at a constant temperature. In this we consider constant heat sources in the flow region. We take P = 0.71. The problem is analyzed in the cases, viz wide gap (s=1) and narrow gap (s=0.2). The velocity and temperature has been analyzed for different variables of G,M, D^{-1}, α , and λ are presented in figs. 1-18. The actual axial flow is in the vertically down ward direction and therefore w>0 represents a reversal flow. It is found that the axial velocity is positive in the vicinity of the outer cylinder in both the wide gap and narrow cases. In the heating it appears r =1 in the cooling case and the region of reversal flow enlarges with increase in |G|. Also the magnitude of w experiences an enhancement with increase in |G| (fig. 1&10). The variation of w with Hartman no. M shows that reversal flow of one which appears in a narrow region adjacent to r = 2 reduces in its size with increase in M. |w| depreciates with increase in M every where in the flow region in both wide and narrow gap cases (figs 2&11). The behavior of w with Darcy parameter D^{-1} shows that lesser the permeability of the porous medium smaller the magnitude of w in the entire region (figs 3&12). The variation of w with heat sources parameter α reveals that in the wide gap case the reversal flow appears near the outer cylinder for α = 2 and disappears for higher $\alpha \geq 4$ and it appears in the entire flow zone for any α <0 and the region of reversal flow enlarges with increase in $|\alpha|$><0 while in the narrow gap case it appears near r =1.2 for any $|\alpha|$><0 and its size reduces with α >0 and enhances with α <0. The magnitude of w enhances with increase in $|\alpha|$><0 in a wide gap case while in narrow gap |w| enhances with increase in α >0 and reduces with $|\alpha|$<0. Fig 4&13). The variation w with suction parameter λ shows that w is always negative for any values of α there by indicating that reversal flow does not appear any where in the flow zone for any λ and |w| experiences an enhancement with increase in λ anywhere in the fluid region (fig 5&12).

The non-dimensional temperature distribution (θ) is shown in fig 6-9 in wide gap case and in figs 15-18 in narrow gap cases for different G,M, D^{-1}, α , and λ we follow the convention that the temperature is positive or negative according as actual temperature is greater or lesser than the equilibrium temperature. From (fig 6&15) we find that the temperature is positive for different |G|(><0). An increase in |G|(><0) results in an enhancement in (θ) in the entire

flow zone in a wide gap case while in a narrow gap case it enhances in the vicinity of the inner cylinder and depreciates in the region adjacent to r =1.2 with |G|(<0). The variation of θ with M in a wide gap case the temperature reduces with increase in M while in a narrow gap case θ enhances with M<3 and depreciates with higher $M \geq 4$ (fig 7&16) The behavior of θ with D^{-1} shows that lesser the permeability of the porous medium larger θ in the wide gap case and smaller θ in the narrow gap case. Also an increase in the suction parameter λ reduces the actual temperature in the entire flow region in both wide gap and narrow gap case (fig 8 & 17). The variation of θ with heat source parameter α shows that $\theta > 0$ for $\alpha > 0$ and $\theta < 0$ for $\alpha < 0$. Also it is found that the actual temperature experiences an enhancement with increase in the strength of heat source/sinks (fig 9&18). In general we notice that the non-dimensional temperature in the wide gap case is larger than that in the narrow gap case.

The shear stress and the rate of heat transfer at the inner and outer cylinders have been evaluated for different G, M, D^{-1}, α and λ are presented in tables 1-12. It is found that the stress at r =1 is negative in the heating case and positive in the cooling case in both wide gap and narrow gap cases.$|\tau|$ enhances with increase in |G|(><0). An increase in M or D^{-1} leads to a depreciation in $|\tau|$ at r =1. Also $|\tau|$ reduces with increase in the suction parameter λ . In variation of τ with heat sources parameter α indicates that $|\tau|$ enhances with $\alpha > 0$ and reduces with $|\alpha|$ (<0) in both the cases (table 2, 4, 10 & 12). At the outer cylinder $|\tau|$ enhances with |G| (><0) in the wide gap case while in narrow gap case $|\tau|$ depreciates with $G \leq 4$ and enhances with higher $G \geq 6$. An increase in M ≤ 3 reduces $|\tau|$and enhances with higher $M \geq 6$. An increase in $M \leq$ reduces $|\tau|$ and enhances with higher $M \geq 5$ in wide gap case while in a narrow gap case it enhances with M (Table 3). The variation of τ with D^{-1} indicates that lesser the permeability of the porous medium smaller $|\tau|$ in both the cases. An increase in the suction parameter λ enhances $|\tau|$ in the wide gap case and reduces it in the narrow gap case. Also $|\tau|$ experiences an enhancement with increase in the strength of the heat sources/sinks (table 2&4) in both the cases.

The Nusselt number (non-dimensional) measures the rate of heat transfer at the boundaries has been evaluated for different G, M, D^{-1}, α , and λ presented in (tables 5 & 6) in wide gap case and (11 & 12) in narrow gap case. It is found that the rate of heat transfer at r = 1 depreciates in the wide gap and enhances in the narrow gap with increase |G. An increase in $M \leq 3$ enhances |Nu| and reduces with higher $M \geq 5$ in wide gap case and reduces in the narrow gap case (table 5 & 12). The variation of Nu with D^{-1} shows that lesser the permeability of the porous medium smaller |Nu| at r =1 at both the cases. Also an increase in the suction parameter λ reduces |Nu| in both wide gap and narrow gap cases. An increase in the heat sources parameter $\alpha \leq 4$ reduces |Nu| and enhances for higher $\alpha \geq 6$ in the wide gap case and reduces for all ($\alpha > 0$) in the narrow gap case while an increase in $|\alpha|$(<0) enhances |Nu| in both wide gap and narrow gap cases (table 6 & 12). In general the rate of heat transfer at r =1 in the narrow gap case is larger than that in the wide gap case.

REFERENCES

1	Al-Nimir,M.A	Analytical solution for transient laminar fully developed free convection in vertical concentric annuli. , Int. J. Heat and Mass transfer, V.36, pp.2388-2395	1993
2	Antonio Barletta	combined forced and free convection with viscous dissipation in a vertical circular duct. , Int. J Heat and Mass Transfer, V.42, pp.2243-2253	1999
3	Arti Lalchandani, and Sarvadeshik	Delhi, Dec.8.p.5	2002
4	Caltigirone , J.P	Thermoconvective instabilities in a porous medium bounded by two concentric horizontal cylinder. , J. Fluid Mech, V.76, pp.337-362.	1996
5	Chandrasekhar,B.C., Nagaraju.P,	Heat transfer in the case of a steady laminar flow of a gray fluid with small optical density past a horizontal plate embedded in a porous medium, waemw, Stoftubertras, vol.23 (6)pp.243-352	1998
6	El-Shaarawi.M.A and Al-Nimr,M.A	Fully developed laminar natural convection in open ended vertical concentric annuli. , Int. J. Heat and Mass Transfer, pp.1873-1884.	1990
7	Faces,N and Farout,B	ASME.J.Heat Transfer,V.105,p.680	1983
8	Havstad,M.A and Burns,P.J	Convective heat transfer in vertical cylindrical annuli filled with a porous medium. , Int. J Heat and mass transfer. V.25.No.11, pp.1755-1766	1982
9	Hossian M.A., Alim M.A,	natural convection radiation interaction on boundary layer flow along a thin vertical cylinder , Heat and mass transfer 32,1515-1520	1997
10	Irfan Anjum Baruddin et al	Effect of viscous dissipation and radiation on natural convection in a porous medium embedded with in vertical annulus, International Journal of thermal sciences 46,221-227.	2007
11	Jain, S.C., et al.,	diabetes Res.Clin.Pract. 9(1), 69	1983
12	Lachman,G.V	Vol.1 & 2.,Pergamon press	1961
13	Loewe, et al.,	Cult.Med.Psyphiatry,24(4),379	2000

14	Mihirsen and Torrance, K.E	natural convection in thin horizontal porous annulus. , Int. J Heat and mass Transfer, V.30, No.4, p.729,	1987
15	Mohammadien,A.A and El.Amin M.E.,	Thermal radiation effects on power-law fluids over a horizontal plates embedded in a porous medium, Int. Comm. Heat Mass, vol. 27 (2) pp.1025-1035.	2000
16	Nguyen,T.H, Satish,M.G, Robollard,L and Vasseur,P	Heat transfer in porous media particulate flows,HTD-V.46.,p.41.the Ame. Soc. Mec. Engg, New Yark,	1985
17	Ostrele,J.F and Young,F.IL	Natural convection between heated vertical plates in a horizontal magnetic field Fluid Mech., V.11, pp.512-518,	1961
18	Philip,J.R	Axisymmetric free convection at small Rayleigh numbers in porous cavities., Int. J. Heat and Mass Transfer, V,25, pp.1689-1699,	1982
19	Poots,G	Laminar natural convection flow in magneto-hydrodynamics., Int. J Heat and mass Transfer,V.3,No.1,pp.1-25,	1961
20	Prasad,V,and Kulacki,F.A and Keyhani,M	Natural convection in porous media. Int. J fluid Mech., V. 150, pp. 89-119	1985
21	Prasad,V	: Natural convection in porous media. , Ph. D thesis	1983
22	Prasad,Vand Kulacki,F.A	Natural convection in a vertical porous annulus. Int. J Heat and mass Transfer,V.27,No.2,pp.207-219,	1984
23	Rajamani R.C.,SreenivasC.,Nithiar asu P.,Seetharamu K.N.,	connective heat transfer in axisymetric porous bodies, International journal of numerical methods for heat and fluid flow.5, 829-837.	1995
24	Rao Yan:Fei,Tasutoni Miki ,Kenji Fukuda,Yasuyuki Takata and Shu Hasegawa	Flow pattern of natural convection in horizontal cylindrical annuli ., Int. J Heat and Mass Transfer, V.28, No.3, pp.705-714,	1985
25	Raptis,A.A.,	Radiation and flow through a porous medium, J. Porous media,Vol4, pp.271-273.	2001
26	Robillard,L Nguyen,T.H,Sathish,M.	Heat transfer in porous media in particulate flows,The Ame.soc.Mech.Engg.,	1985

	G and Vassueur,P	HTD-V.46,p.412,New York,	
27	Ronald,A.,Fisher and Fornk Yates ,	Statistical tables (for biological agricultural and medicinal research),Longman	1979
28	Sastry, V.U.K and Bhadram, C.V.V;	App.Sci.Res, 34, V.213, p.117,	1978
29	Singh, K.R and Cowling,T.J	Thermal convection in magneto hydrodynamics, Quart. J Mech. and Appl.Maths,V.16,pp.1-15,	1963
30	Sivanjaneya Prasad,P	Effects of convection Heat and mass transfer in unsteady hydro magnetic channel flows. , Ph. D thesis. S.K.Univercity, Anantapur, India,	2001
31	Sree Ramachandra Murthy,A	Buoyancy induced hydro magnetic flows through a porous medium-A study ,Ph. D thesis. , S.K. Univercity, Anantapur, India,	1992
32	Yih ,K.A.,	Radiation effect on natural convection over a vertical cylinder embedded in a porous media, International communication in heat and mass transfer 26 , 1025-1035.	1999
33	Yu,C.P and Yung,W	Effects of wall conductance on convective magneto Hydrodynamic channel flow. Appl.Sci.Res., V.20, p.16,	1969
34	Yu,C.P	Convective magneto -hydrodynamic flow in a vertical channel., Appl. Sci. Res., V.22, p.127,	1970

PUNE RESEARCH WORLD ISSN 2455-359X
AN INTERNATIONAL JOURNAL OF INTERDISCIPLINARY STUDIES VOL 2, ISSUE 2

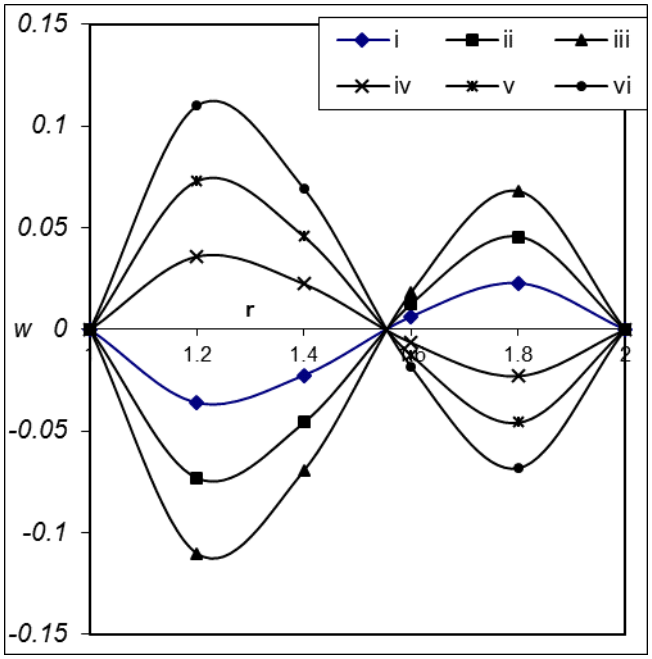

M = 2, $D^{-1} = 10^2$, $\lambda = 0.2$, $\alpha = 2$, N=1, E_c =0.01

	i	ii	iii	iv	v	vi
G	10^3	3×10^3	5×10^3	-10^3	-3×10^3	-5×10^3

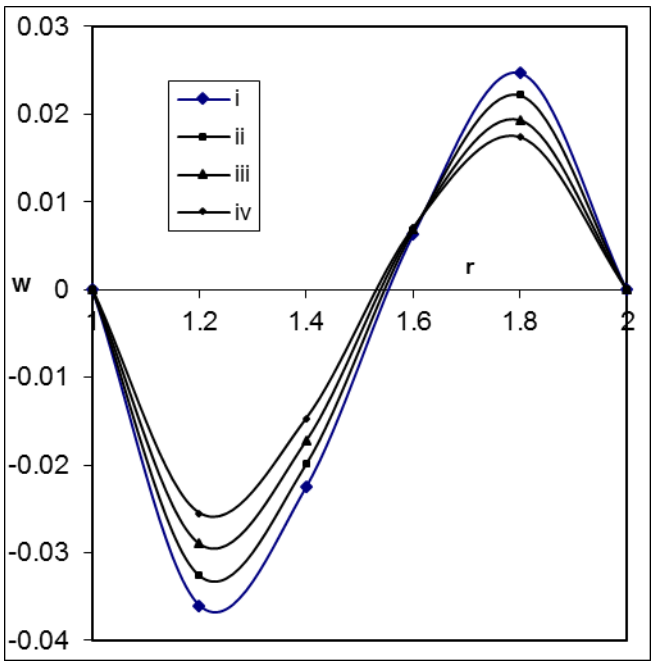

Figure 1. Axial velocity w with G

$M = 2,\ D^{-1} = 10^2,\ \lambda = 0.2,\ \alpha = 2, N=1, E_c = 0.01$

	i	ii	iii	iv	v	vi
G	10^3	3×10^3	5×10^3	-10^3	-3×10^3	-5×10^3

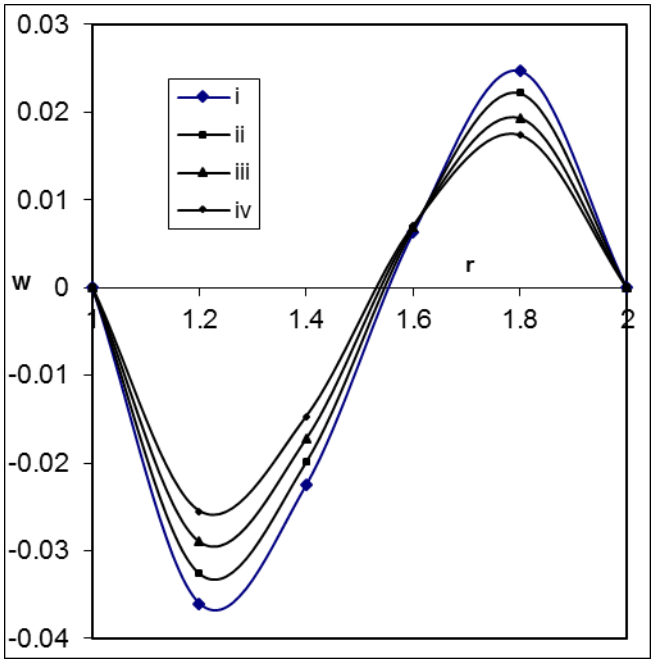

Figure 2. Velocity w with M

$G = 10^3,\ D^{-1} = 10^2,\ \lambda = 0.2,\ \alpha = 2, N=1, E_c = 0.01$

	i	ii	iii	iv
M	2	4	6	10

PUNE RESEARCH WORLD ISSN 2455-359X
AN INTERNATIONAL JOURNAL OF INTERDISCIPLINARY STUDIES VOL 2, ISSUE 2

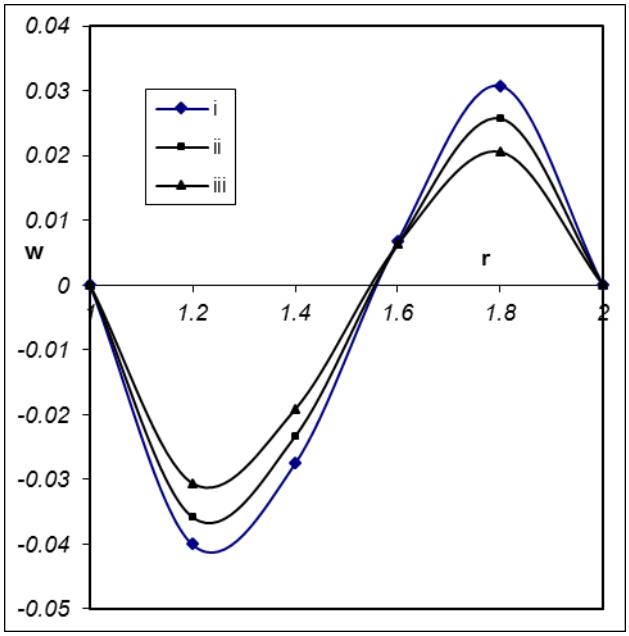

Figure 3. Velocity w with D^{-1}

G = 10^3, M = 2, λ =0.2, α =2, N=1, E_c =0.01

	i	ii	iii
D^{-1}	10^2	3×10^2	5×10^2

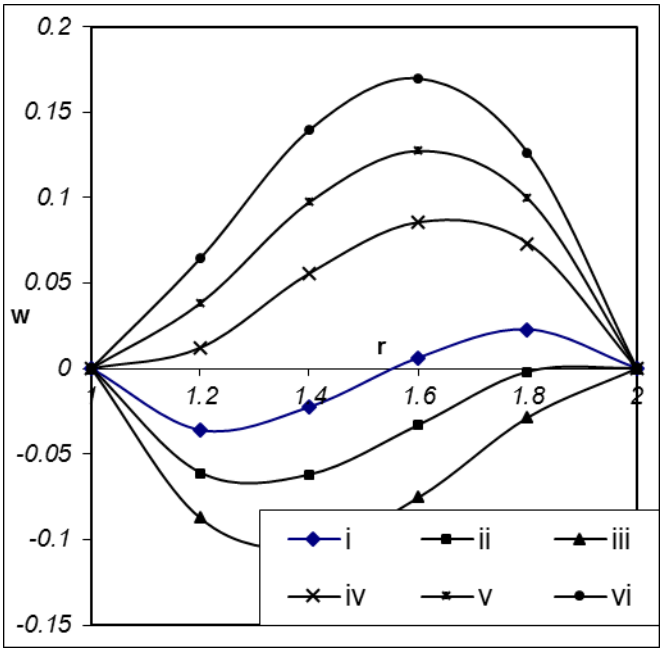

Figure 4. Velocity w with α

G = 10^3, M = 2, D^{-1} = 10^2, λ =0.2, N=1, E_c =0.01

	i	ii	iii	iv	v	vi
α	2	4	6	-2	-4	-6

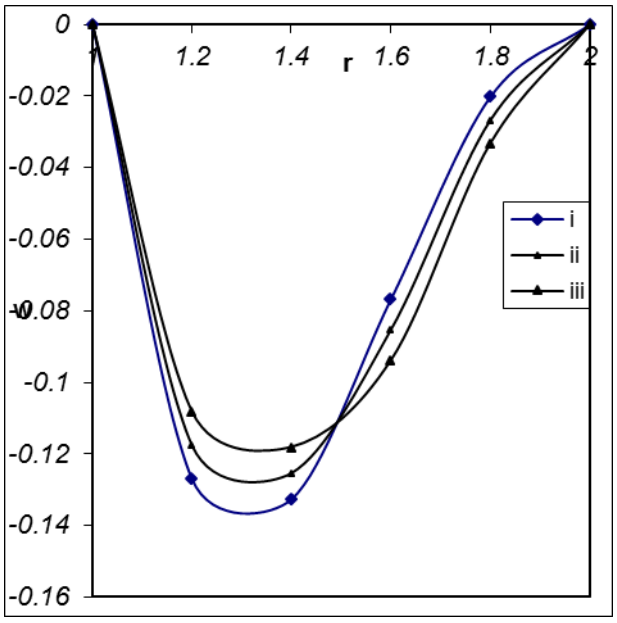

Figure 5. Velocity w with λ

G = 10^3, M = 2, $D^{-1} = 10^2$, α =2, N=1, E_c =0.01

	i	ii	iii
λ	0.2	0.4	0.6

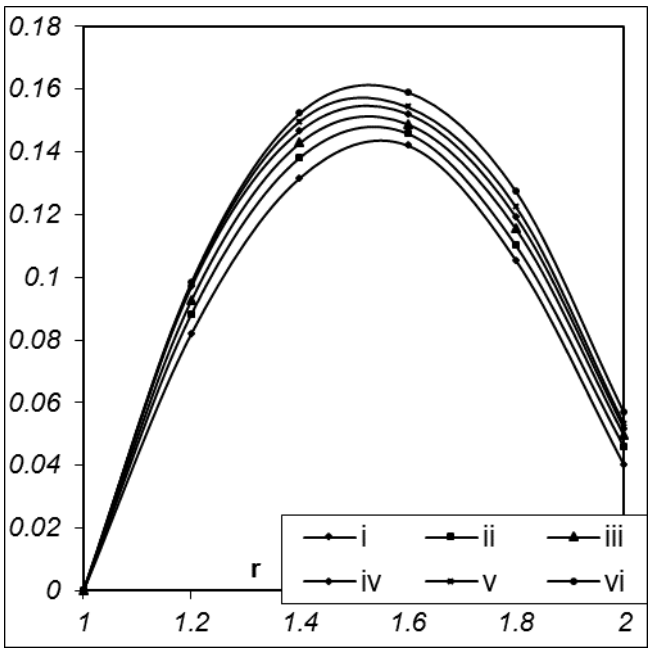

Figure 6. Temperature θ with G

M = 2, $D^{-1} = 10^2$, λ =0.2, α =2,N=1, E_c =0.01

	i	ii	iii	iv	v	vi
G	10^3	3×10^3	5×10^3	-10^3	-3×10^3	-5×10^3

PUNE RESEARCH WORLD ISSN 2455-359X
AN INTERNATIONAL JOURNAL OF INTERDISCIPLINARY STUDIES VOL 2, ISSUE 2

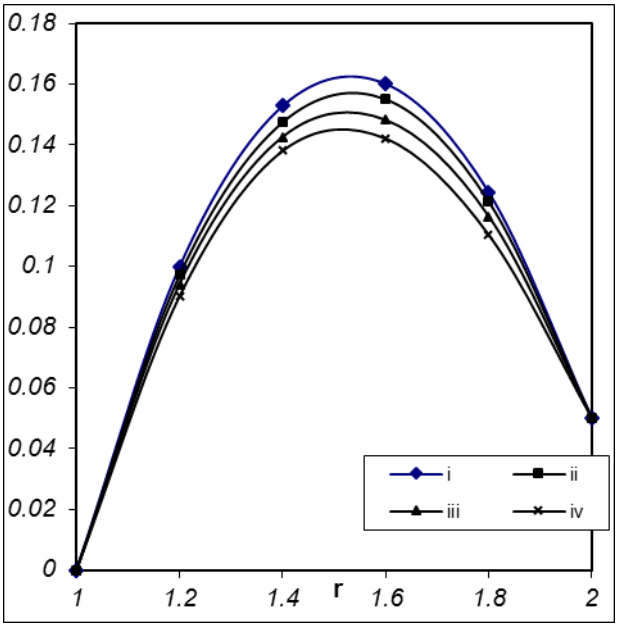

Figure 7. Temperature θ with M

$G = 10^3$, $D^{-1} = 10^2$, $\lambda = 0.2$, $\alpha = 2$, $N = 1$, $E_c = 0.01$

	i	ii	iii	iv
M	2	4	6	10

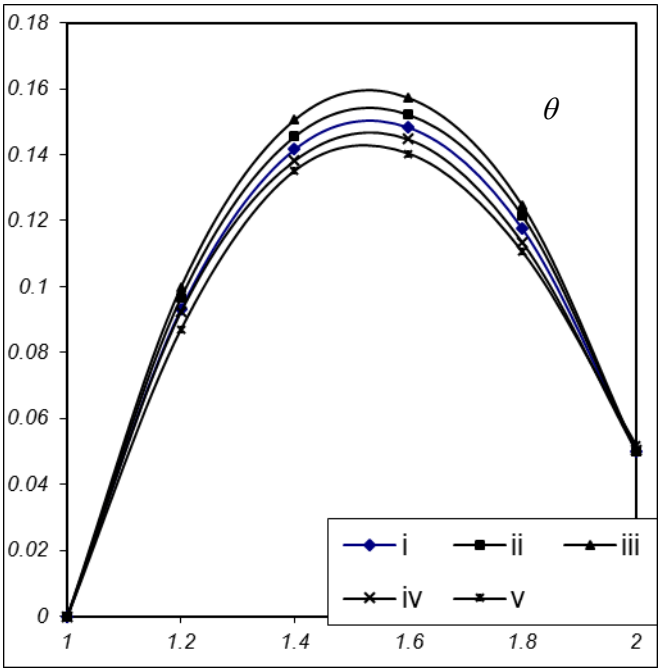

Figure 8. Temperature θ with D^{-1} & λ

$G = 10^3$, M = 2, α =2, N=1, E_c =0.01

	i	ii	iii	iv	v
D^{-1}	10^2	3×10^2	5×10^2	10^2	10^2
λ	0.2	0.2	0.2	0.4	0.6

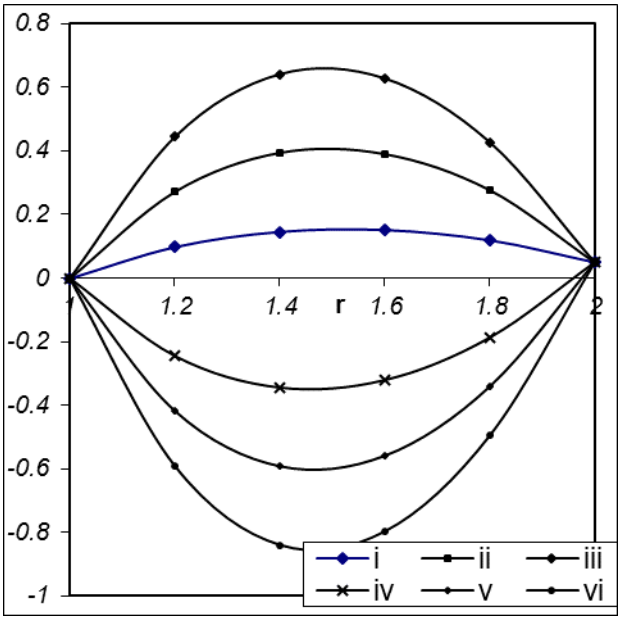

$G = 10^3$, M = 2, $D^{-1} = 10^2$, λ =0.2, N=1, E_c =0.01

	i	ii	iii	iv	v	vi
α	2	4	6	-2	-4	-6

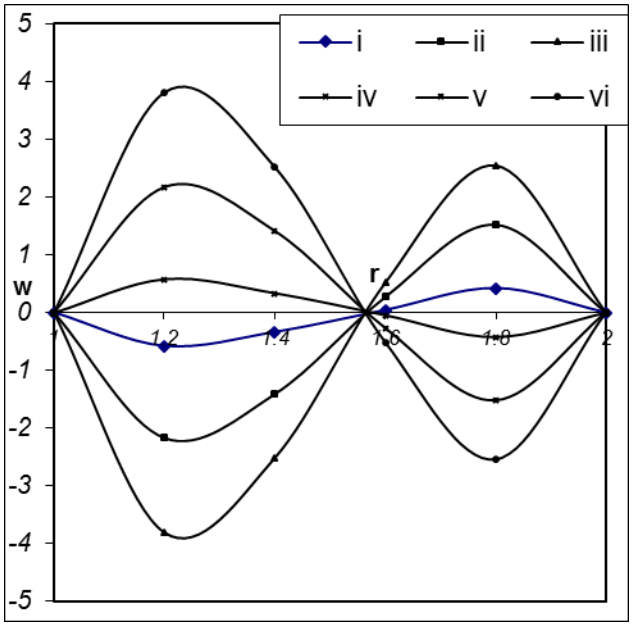

Figure 10. Velocity w with G

M = 2, $D^{-1} = 10^2$, $\lambda = 0.2$, $\alpha = 2$, N=1, E_c =0.01

	i	ii	iii	iv	v	vi
G	10^3	3×10^3	5×10^3	-10^3	-3×10^3	-5×10^3

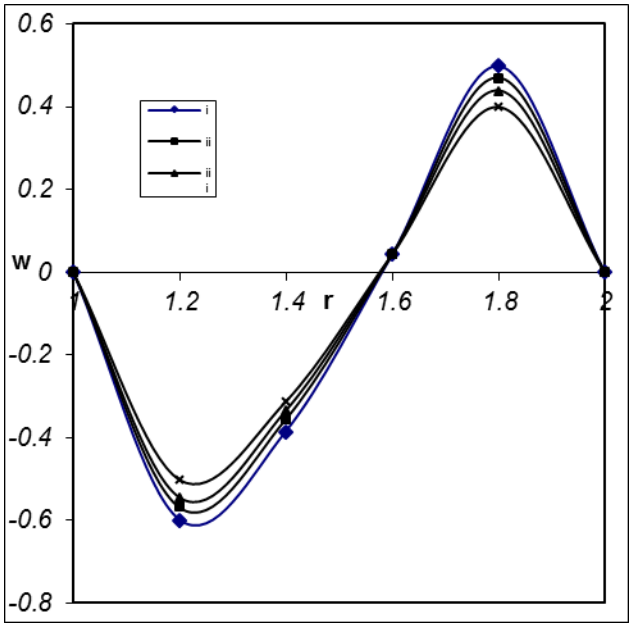

Figure 11. Velocity w with M

$G = 10^3$, $D^{-1} = 10^2$, λ =0.2, α =2, N=1, E_c =0.01

	i	ii	iii	iv
M	2	4	6	10

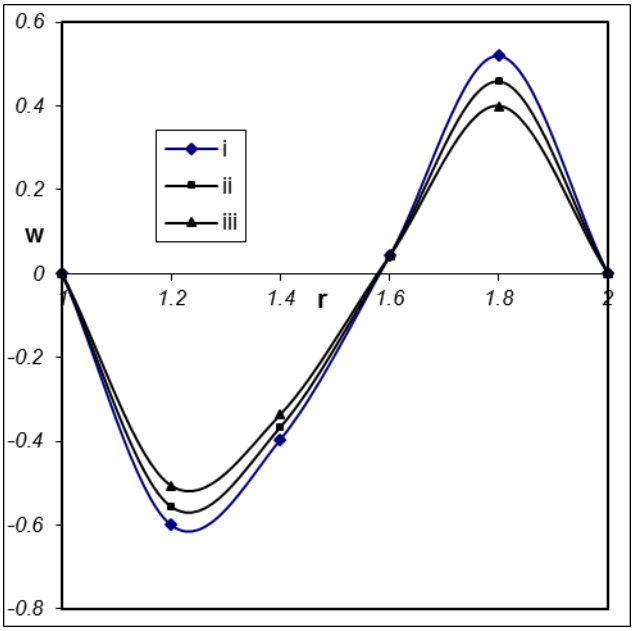

Figure 12. Velocity w with D^{-1}

G = 10^3, M = 2, α =2, N=1, E_c =0.01

	i	ii	iii	iv	v
D^{-1}	10^2	3×10^2	5×10^2	10^2	10^2

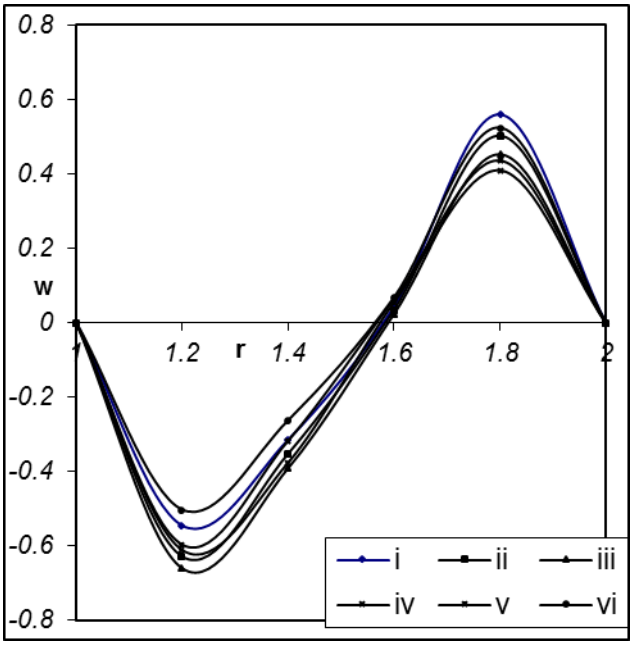

Figure 13. Velocity w with α

G = 10^3, M = 2, D^{-1} = 10^2, λ =0.2, N=1, E_c =0.01

	i	ii	iii	iv	v	vi
α	2	4	6	-2	-4	-6

	i	ii	iii	iv	v	vi
G	10^3	3×10^3	5×10^3	-10^3	-3×10^3	-5×10^3

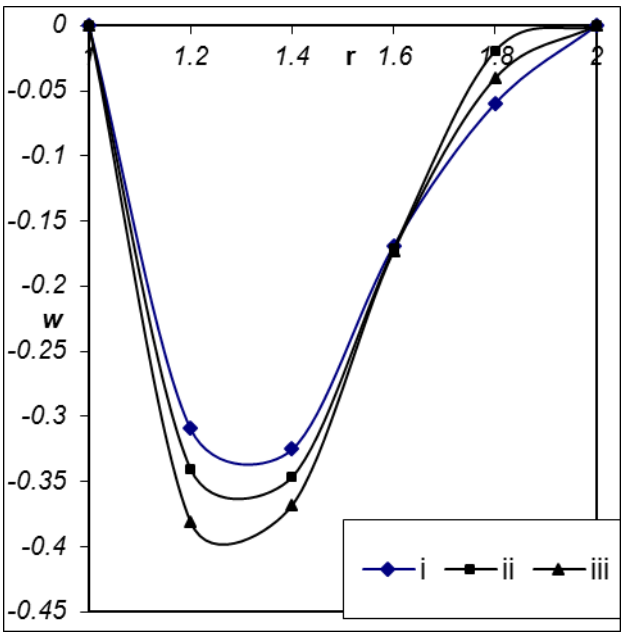

Figure 14. Velocity w with λ

G = 10^3, M = 2, $D^{-1} = 10^2$, α =2, N=1, E_c =0.01

	i	ii	iii
λ	0.2	0.4	0.6

θ

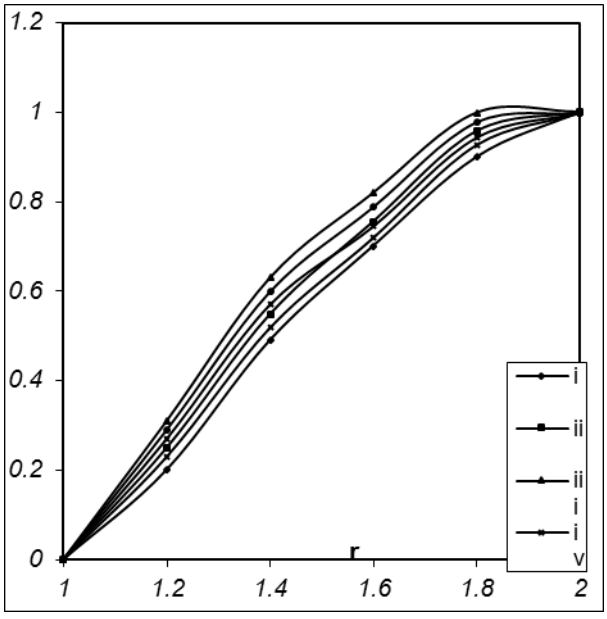

Figure 15. Temperature θ with G

M = 2, $D^{-1} = 10^2$, λ =0.2, α =2,N=1, E_c =0.01

θ

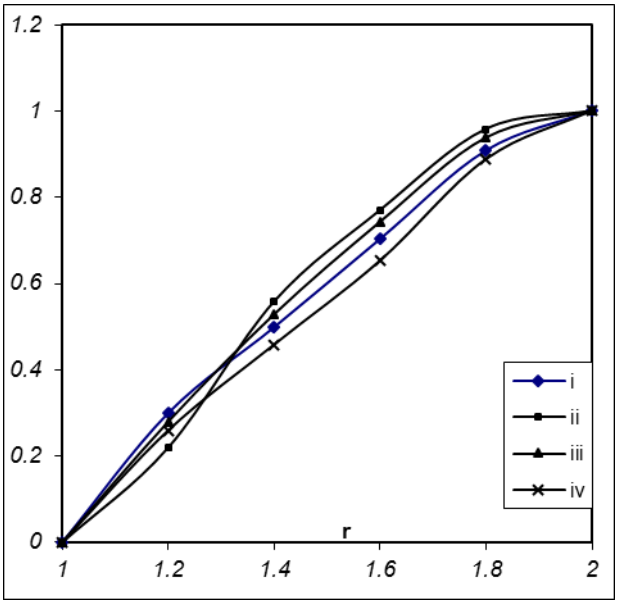

Figure 16. Temperature θ with M

G = 10^3, $D^{-1} = 10^2$, λ =0.2, α =2, N=1, E_c =0.01

	i	ii	iii	iv
M	2	4	6	10

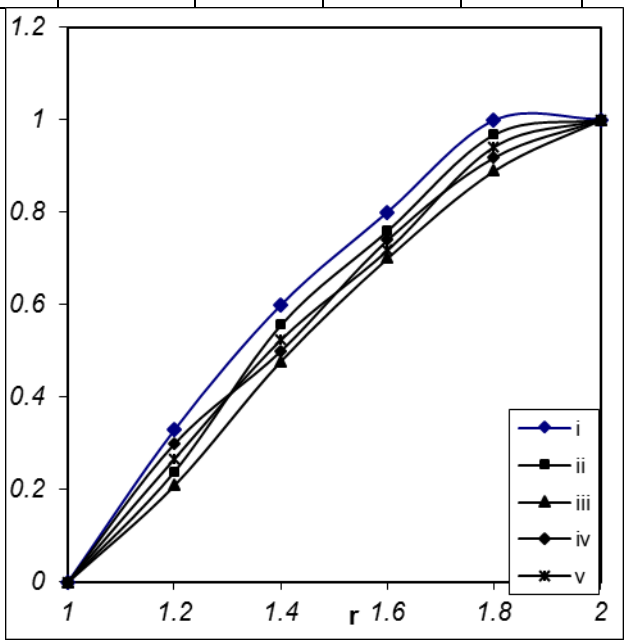

Figure 17. Temperature θ with D^{-1} & λ

$G = 10^3$, M = 2, α =2, N=1, E_c =0.01

	i	ii	iii	iv	v
D^{-1}	10^2	3×10^2	5×10^2	10^2	10^2
λ	0.2	0.2	0.2	0.4	0.6

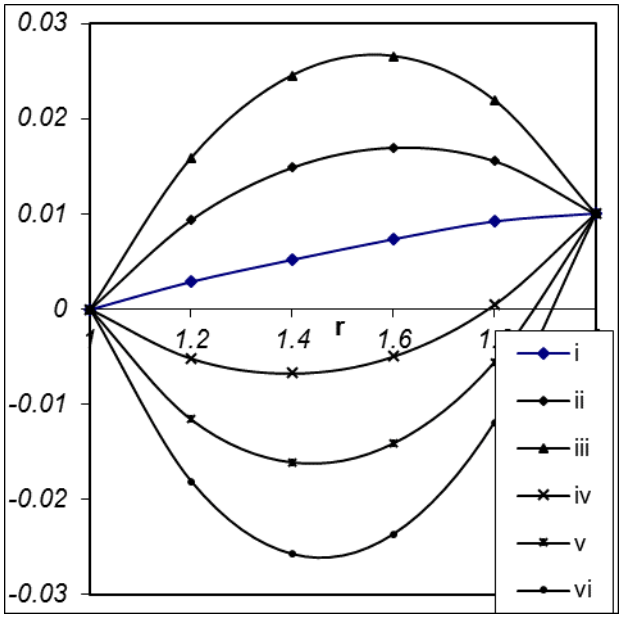

Figure 18. Temperature θ with α

$G = 10^3$, M = 2, $D^{-1} = 10^2$, λ =0.2, N=1, E_c =0.01

	i	ii	iii	iv	v	vi
α	2	4	6	-2	-4	-6

Table – 1

Shear stress $[\tau]_{r=1}$ *at* $s=1$ (*wide gap case*), $\alpha=2$, $N=1$,

G	i	ii	iii	iv	v	vi	vii
10^3	-0.88437	-0.77581	-0.57752	-0.88081	-0.87271	-0.88158	-0.87587
3×10^3	-1.78135	-1.5618	-1.6617	-1077348	-1.75804	-1.77574	-1.76385
5×10^3	-2.67895	-2.34783	-1.74565	-2.66662	-2.64397	-2.67053	-2.65215
-10^3	0.88437	0.77581	0.57752	0.88081	0.87271	0.88158	0.87587
-3×10^3	1.78133	1.56179	1.16169	1.77344	1.75758	1.77571	1.7638
-5×10^3	2.67756	2.34775	1.74555	2.66522	2.6411	2.6697	2.65078
M	2	3	5	2	2	2	2
D^{-1}	10^3	10^3	10^3	3×10^3	5×10^3	10^3	10^3
λ	0.2	0.2	0.2	0.2	0.2	0.3	0.5

Table – 2

Shear stress $[\tau]_{r=1}$ *at* $s=1$ (*wide gap case*), $M=2,\ D^{-1}=10^3, \lambda=0.2, N=1$

G	i	ii	iii	iv	v	vi
10^3	-0.88437	-1.02465	-1.16508	-0.6037	-0.49237	0.35266
3×10^3	-1.78135	-2.06195	-2.34258	-1.21987	-0.97391	-0.69328
5×10^3	-2.67895	-3.09926	-3.5198	-1.83798	-1.45698	-1.0372
-10^3	0.88437	1.02465	1.16507	0.6037	0.49237	0.35265
-3×10^3	1.78133	2.0615	2.34163	1.21974	0.97385	0.6933
-5×10^3	2.67756	3.09659	3.51524	1.83747	1.45671	1.03694
α	2	4	6	-2	-4	-6

Table - 3

Shear stress $[\tau]_{r=1+s}$ *at* $s=1$ (*wide gap case*), $\alpha=2, N=1$

G	i	ii	iii	iv	v	vi	vii
10^3	0.02158	-0.01921	-0.07856	0.01978	0.01555	0.02802	0.04124
3×10^3	0.05146	-0.03149	-0.15229	0.04736	0.03938	0.06454	0.09114
5×10^3	0.08178	-0.04368	-0.22585	0.07570	0.06495	0.10156	0.14149
-10^3	-0.02158	0.01921	0.07855	-0.01978	-0.01555	-0.02801	-0.04123
-3×10^3	-0.05141	0.03150	0.05228	-0.04727	-0.03839	-0.06447	-0.09101
-5×10^3	-0.08013	0.04383	0.22611	-0.07310	-0.05957	-0.10000	-0.13877
M	2	3	5	2	2	2	2
D^{-1}	10^3	10^3	10^3	3×10^3	5×10^3	10^3	10^3
λ	0.2	0.2	0.2	0.2	0.2	0.3	0.5

Table – 4

Shear stress $[\tau]_{r=1+s}$ *at* $s=1$ (*wide gap case*), $M=2,\ D^{-1}=10^3, \lambda=0.2, N=1$

G	i	ii	Iii	iv	v	vi
10^3	0.02158	0.16895	0.31642	-0.27086	-0.40001	-0.54713
3×10^3	0.05146	0.34617	0.64079	-0.53698	-0.80645	-1.10078

5×10^3	0.08178	0.52319	0.9645	-0.79887	-1.20921	-1.64874
-10^3	-0.02158	-0.16892	-0.31636	0.27084	0.39996	0.54707
-3×10^3	-0.05141	-0.34525	-0.63887	0.53704	0.80625	1.10039
-5×10^3	-0.08013	-0.51826	-0.95599	0.79963	1.2094	1.64885
α	2	4	6	-2	-4	-6

Table - 5

Nusselt Number $[Nu]_{r=1}$ *at* $s=1$ (*wide gap case*), $\alpha=2,\ N=1$

G	i	ii	iii	iv	v	vi	vii
10^3	-0.76599	-0.76599	-0.76597	-0.76595	-0.76587	-0.7405	-0.69073
3×10^3	-0.76569	-0.76575	-0.76573	-0.76545	-0.76494	-0.74017	-0.6904
5×10^3	-0.76509	-0.76517	-0.76495	-0.76395	-0.76163	-0.73951	-0.68955
-10^3	-0.76598	-0.766	-0.76598	-0.76594	-0.76585	-0.74049	-0.6907
-3×10^3	-0.76569	-0.7658	-0.7658	-0.76548	-0.76505	-0.74017	-0.69041
-5×10^3	-0.76583	-0.76538	-0.76551	-0.7659	-0.76597	-0.74052	-0.69131
M	2	3	5	2	2	2	2
D^{-1}	10^3	10^3	10^3	3×10^3	5×10^3	10^3	10^3
λ	0.2	0.2	0.2	0.2	0.2	0.3	0.5

Table – 6

Nusselt Number $[Nu]_{r=1}$ *at* $s=1$ (*wide gap case*), $M=2,\ D^{-1}=10^3, \lambda=0.2, N=1$

G	i	ii	iii	iv	v	vi
10^3	-0.76599	0.30921	1.38455	-2.91693	-3.9602	-5.03514
3×10^3	-0.76569	0.39048	1.38448	-2.91535	-3.95725	-5.03132
5×10^3	-0.76509	0.30981	1.38458	-2.91213	-3.95275	-5.02497
-10^3	-0.76598	0.30922	1.38466	-2.91702	-3.96045	-5.03565
-3×10^3	-0.76569	0.30884	1.38326	-2.91628	-3.95858	-5.03325
-5×10^3	-0.76583	0.30688	1.37968	-2.91442	-3.95564	-5.02906
α	2	4	6	-2	-4	-6

Table - 7

Nusselt Number $[Nu]_{r=1+S}$ *at* $s=1$ (*wide gap case*), $\alpha=2,\ N=1$

G	i	ii	iii	iv	v	vi	vii
10^3	-1.22722	-1.22712	-1.22707	-1.22722	-1.22721	-1.24197	-1.27192
3×10^3	-1.22729	-1.22715	-1.22706	-1.22732	-1.22743	-1.24206	-1.27205
5×10^3	-1.22743	-1.22727	-1.22698	-1.22743	-1.2274	-1.24221	-1.27214
-10^3	-1.22713	-1.22721	-1.22727	-1.22713	-1.22715	-1.24187	-1.27189
-3×10^3	-1.22723	-1.22724	-1.22732	-1.22731	-1.22746	-1.24201	-1.27204
-5×10^3	-1.22763	-1.22734	-1.22737	-1.22795	-1.22856	-1.2425	-1.27287
M	2	3	5	2	2	2	2
D^{-1}	10^3	10^3	10^3	3×10^3	5×10^3	10^3	10^3
λ	0.2	0.2	0.2	0.2	0.2	0.3	0.5

Table – 8

Nusselt Number $[Nu]_{r=1+S}$ *at* $s=1$ (*wide gap case*), $M=2,\ D^{-1}=10^3, \lambda=0.2, N=1$

G	i	ii	iii	iv	v	vi
10^3	-1.22722	-2.15247	-3.07778	0.62369	1.52866	2.45383
3×10^3	-1.22729	-2.15273	-3.0783	0.62407	1.5291	2.45472
5×10^3	-1.22743	-2.15317	-3.07911	0.62492	1.53036	2.45621
-10^3	-1.22713	-2.15221	-3.07746	0.62337	1.5283	2.45341
-3×10^3	-1.22723	-2.15265	-3.07834	0.62351	1.52844	2.45393
-5×10^3	-1.22763	-2.15373	-3.08011	0.62395	1.52922	2.45483
α	2	4	6	-2	-4	-6

Table – 9

Shear stress $[\tau]_{r=1}$ *at* $s=0.2$ (*narrow gap case*), $\alpha=2,\ N=1,$

G	i	ii	iii	iv	v	vi	vii
10^3	-0.1341	-0.13132	-0.13016	-0.13409	-0.13408	-0.13402	-0.13305
3×10^3	-0.33451	-0.33095	-0.32208	-0.33447	-0.3344	-0.3343	-0.33387
5×10^3	-0.53638	-0.53316	-0.51611	-0.53631	-0.53617	-0.53787	-0.53721
-10^3	0.1341	0.13132	0.13016	0.13409	0.13408	0.13402	0.13305
-3×10^3	0.33451	0.33095	0.32208	0.33447	0.3344	0.3343	0.33387
-5×10^3	0.53638	0.53316	0.51611	0.53631	0.53617	0.53787	0.53721
M	2	3	5	2	2	2	2
D^{-1}	10^3	10^3	10^3	3×10^3	5×10^3	10^3	10^3
λ	0.2	0.2	0.2	0.2	0.2	0.3	0.5

Table – 10

Shear stress $[\tau]_{r=1}$ *at* $s=0.2$ (*narrow gap case*), $M=2,\ D^{-1}=10^3, \lambda=0.2, N=1$

G	i	ii	iii	iv	v	vi
10^3	-0.1341	-0.1345	-0.13489	-0.13093	-0.13056	-0.13018
3×10^3	-0.33451	-0.33597	-0.33936	-0.32968	-0.3263	-0.3249
5×10^3	-0.53638	-0.54087	-0.54534	-0.53107	-0.52841	-0.52221
-10^3	0.1341	0.1345	0.13489	0.13093	0.13056	0.13018
-3×10^3	0.33451	0.33597	0.33936	0.32968	0.3263	0.3249
-5×10^3	0.53638	0.54887	0.54534	0.53107	0.52841	0.52221
α	2	4	6	-2	-4	-6

Table – 11

Shear stress $[\tau]_{r=1+s}$ *at* $s=0.2$ (*narrow gap case*), $\alpha=2, N=1$

G	i	ii	iii	iv	v	vi	vii
10^3	-0.01509	-0.01592	-0.01611	-0.01506	-0.01504	-0.0169	-0.01852
3×10^3	0.00183	-0.00004	-0.00435	0.00182	0.00179	0.00246	0.00372
5×10^3	0.02632	0.02477	0.01504	0.02628	0.02621	0.02874	0.03098
-10^3	0.01509	0.01592	0.01611	0.01505	0.01502	0.0149	0.01452
-3×10^3	-0.00183	0.00004	0.00435	-0.00182	-0.00179	-0.00246	-0.00372
-5×10^3	-0.02632	-0.02477	-0.01504	-0.02628	-0.02621	-0.02874	-0.03098
M	2	3	5	2	2	2	2
D^{-1}	10^3	10^3	10^3	3×10^3	5×10^3	10^3	10^3
λ	0.2	0.2	0.2	0.2	0.2	0.3	0.5

Table – 12

Shear stress $[\tau]_{r=1+s}$ *at* $s=0.2$ (*narrow gap case*), $M=2$, $D^{-1}=10^3$, $\lambda=0.2$, $N=1$

G	i	ii	iii	iv	v	vi
10^3	-0.01509	-0.01437	-0.01365	-0.01726	-0.01797	-0.01866
3×10^3	0.00183	0.00386	0.00713	-0.00342	-0.00663	-0.0086
5×10^3	0.02632	0.03105	0.03575	0.01952	0.01612	0.01021
-10^3	0.01509	0.01437	0.01365	0.01726	0.01797	0.01866
-3×10^3	-0.00183	-0.00386	-0.00713	0.00342	0.00663	0.0086
-5×10^3	-0.02632	-0.03105	-0.03575	-0.01952	-0.01612	-0.01021
α	2	4	6	-2	-4	-6

Table – 13

Nusselt Number $[Nu]_{r=1}$ *at* $s=0.2$ (*narrow gap case*), $\alpha=2$, $N=1$

G	i	ii	iii	iv	v	vi	vii
10^3	-5.31018	-5.30018	-5.28018	-5.28018	-5.26018	-5027761	-5.21289
3×10^3	-5.32018	-5.31018	-5.30018	-5.30018	-5.28018	-5027761	-5.21289
5×10^3	-5.33018	-5.32018	-5.31018	-5.31018	-5.30017	-5027761	-5.21289
-10^3	-5.30018	-5.28018	-5.26018	-5.29018	-5.26018	-5027761	-5.21289
-3×10^3	-5.31018	-5.29018	-5.28018	-5.30018	-5.29018	-5027761	-5.21289
-5×10^3	-5.32018	-5.30018	-5.30018	-5.32018	-5.30017	-5027761	-5.21289
M	2	3	5	2	2	2	2
D^{-1}	10^3	10^3	10^3	3×10^3	5×10^3	10^3	10^3
λ	0.2	0.2	0.2	0.2	0.2	0.3	0.5

Table – 14

Nusselt Number $[Nu]_{r=1}$ *at* $s=0.2$ (*narrow gap case*), $M=2,\ D^{-1}=10^3, \lambda=0.2, N=1$

G	i	ii	iii	iv	v	vi
10^3	-5.31018	-5.11468	-4.92092	-5.7011	-5.89653	-6.09017
3×10^3	-5.31018	-5.11468	-4.92091	-5.7011	-5.89653	-6.09017
5×10^3	-5.31018	-5.11468	-4.92091	-5.7011	-5.89653	-6.09017
-10^3	-5.31018	-5.11468	-4.92092	-5.7011	-5.89653	-6.09017
-3×10^3	-5.31018	-5.11468	-4.92091	-5.7011	-5.89653	-6.09017
-5×10^3	-5.31018	-5.11468	-4.92091	-5.7011	-5.89653	-6.09017
α	2	4	6	-2	-4	-6

Table – 15

Nusselt Number $[Nu]_{r=1+s}$ *at* $s=0.2$ (*narrow gap case*), $\alpha=2,\ N=1$

G	i	ii	iii	iv	v	vi	vii
10^3	-4.70887	-4.70887	-4.70887	-4.70867	-4.70847	-4.07317	-4.77760
3×10^3	-4.70894	-4.70893	-4.70891	-4.70864	-4.70844	-4.73180	-4.77767
5×10^3	-4.70903	-4.70902	-4.70899	-4.70063	-4.70803	-4.73189	-4.77777
-10^3	-4.70899	-4.70899	-4.70899	-4.70869	-4.70849	-4.73184	-4.77771
-3×10^3	-4.70892	-4.70893	-4.70895	-4.70862	-4.70842	-4.73173	-4.77764
-5×10^3	-4.08830	-4.70884	-4.70888	-4.70843	-4.70823	-4.73168	-4.77754
M	2	3	5	2	2	2	2
D^{-1}	10^3	10^3	10^3	3×10^3	5×10^3	10^3	10^3
λ	0.2	0.2	0.2	0.2	0.2	0.3	0.5

Table – 16

Nusselt Number $[Nu]_{r=1+s}$ *at* $s=0.2$ (*narrow gap case*), $M=2,\ D^{-1}=10^3, \lambda=0.2, N=1$

G	i	ii	iii	iv	v	vi
10^3	-4.70887	-4.89755	-5.08492	-4.33157	-4.14294	-3.95567
3×10^3	-4.70894	-4.89762	-5.085	-4.33162	-4.14298	-3.95571
5×10^3	-4.70903	-4.89772	-5.08511	-4.33171	-4.14307	-3.95578
-10^3	-4.70899	-4.89766	-5.08503	-4.3317	-4.14308	-3.95581
-3×10^3	-4.70892	-4.89759	-5.08495	-4.33165	-4.14303	-3.95577
-5×10^3	-4.0883	-4.89749	-5.08484	-4.33156	-4.14295	-3.95571
α	2	4	6	-2	-4	-6